

Development of a Triglidge-Robot with Enlarged Workspace

C. Budde, P. Last and J. Hesselbach, *Member, IEEE*

Abstract—Despite of a promising potential robots based on parallel kinematic structures have not yet found their way into industry on a large scale. One of the main reasons for that is a workspace to installation-space ratio, which usually is inferior to that of their serial counterparts. In this paper development and design issues of a Triglidge-robot based on the Linear Delta are presented. Using a workspace enlargement approach based on the use of several workspaces going along with different assembly modes of the structure's the workspace to installation-space ratio of this robot can be enhanced significantly. Additionally this paper is part of a joint effort of several authors to benchmark different kinematic structures using based-fixed linear drives against each other. Thus, the presented structure is characterized using standardized benchmark criteria.

I. INTRODUCTION

MANY applications in the field of production automation (material handling, assembly, etc.) require high operating speeds and accelerations. This affects the design of machines for such applications, making new technical solutions necessary to meet the named requirements. In recent years machines for handling and assembly based on parallel kinematic structures have been studied extensively on account of their promising potential for highly dynamic movement. This is due to the possibility to position the machine's drives in the base, resulting in low moved masses. Nevertheless only a few of these machines have found their way into industrial application. Reasons for this are a small orientation range (in machines with rotational degrees of freedom (dof)) and a ratio of workspace to installation-space that is significantly lower than in conventional machines based on serial kinematic structures.

Fortunately the latter drawback does not apply to all parallel structures in equal measure. For structures with linear drives and a parallel arrangement of the drives' axes the extension of the workspace in the direction of the drives' axes is only limited by the positioning range of the drives. Several structures and prototypes using this build-up have been described, e.g. the Linear Delta [1], Triaglidge [2], Linapod [3], Urane SX [4], or Gantry-Tau [5]. This layout

allows for long drawn-out workspaces. But it is only a small step towards a better workspace to installation-space ratio, since larger positioning ranges of the drives lead to larger bases and thus to larger installation-spaces.

A more sophisticated approach is to enlarge the workspace without extending the drives' positioning ranges. This can be accomplished by using several workspaces going along with different solutions of the direct kinematic problem (known as assembly modes). The most simple way to reach two different assembly modes is proposed by Brogardh [5]: The driven carriages carry two identical structures, each with its own endeffector and each mounted in a different assembly mode. Drawbacks to this approach are the higher moved mass and higher cost of two structures and the fact that each endeffector can only reach the workspace of one assembly mode. Thus, it is more effective to change the assembly mode of one structure. To do this it is necessary to pass singular positions of the parallel structure. Theoretical examinations on such a singular change of assembly mode have been done by Nenchev [6] and Wenger [7], but without consideration of the practical implementation in a physical robot. For a planar structure such an implementation has been described in [8] showing that the approach to use the workspaces of several assembly modes can be successfully used to gain a larger overall workspace. For spatial movements several structures are proposed in [5] allowing for the use of different workspaces, which are either of unequal size or feature a different platform orientation.

The aim of this paper is to present optimization and design issues of a Triglidge-robot (based on the Linear Delta). This spatial robot is capable of changing its assembly mode making the use of two symmetrical workspaces possible without a change in platform orientation. The resulting overall workspace for an unchanged installation space leads to an enhanced ratio of workspace to installation-space. Additionally, this paper is part of a joint effort of several authors to compare different parallel kinematic structures with linear drives (some of them named above). To allow for this the used kinematic structure is characterized using standardized benchmark criteria.

II. KINEMATIC STRUCTURE OF PROTOTYPE

The Triglidge-structure like the Linear Delta [1] is built up of three kinematic chains each driven by a linear motor. The parallel arrangement chosen for the linear motors is similar to one used for the machine tool Quickstep [9]. Together these chains guide the working platform (see Fig. 1). Due to the use of two parallel rods for the build-up of each chain the

Manuscript received September 15, 2006. This work was funded by the German Research Foundation (DFG) within the framework of the Collaborative Research Center SFB 562 'Robotic Systems for Handling and Assembly'. The authors would like to thank the DR. JOHANNES HEIDENHAIN GmbH, Traunreut (Germany) for its generous support of the prototype development by supplying the necessary linear encoders.

All authors are with the Institute of Machine Tools and Production Technology, Technical University Braunschweig, Germany (phone +49-531-3917601; fax +49-531-3915842; email {ch.budde, p.last, j.hesselbach}@tu-bs.de)

platform is kept at constant orientation, always. The chains allow for a translational movement of the platform with three dof. To realize an additional rotation around the z-axis a serial axis is added to the platform. Thus, the complete structure is of a hybrid type, consisting of a parallel part and a serial part. Its four dof make the classical Scara-motions possible, which are necessary for the better part of handling and assembly operations.

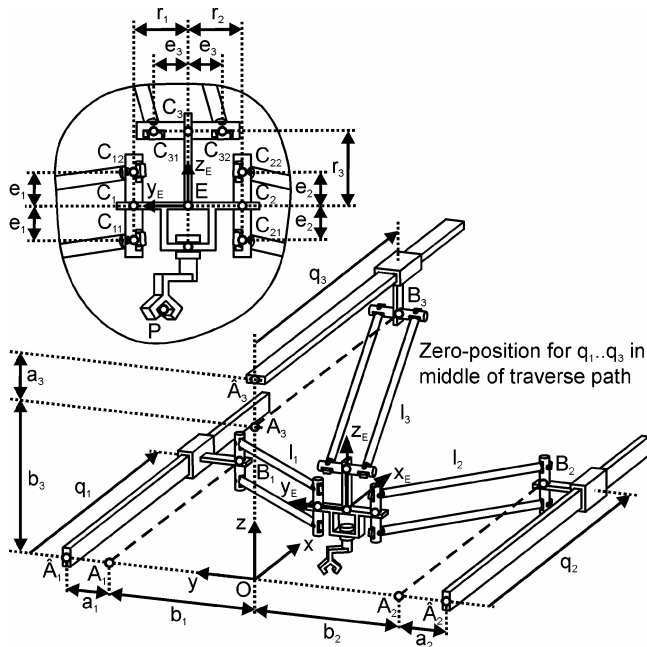


Fig. 1. Kinematic structure of Triglidge-robot.

III. WORKSPACE ENLARGEMENT

The named approach to enlarge the workspace is based on the idea to use several workspaces. These workspaces go along with different working and assembly modes of a parallel kinematic structure, which are defined as follows. Working modes are the different solutions to the inverse kinematic problem (IKP) [10], providing the necessary drive positions for a desired pose of the robot's endeffector. They are divided by singularities of first type, which occur when a kinematic chain of the structure is either in a stretched position or the links of the chain are folded upon each other [11]. In such a singular position, at least one actuator can fulfill an infinitesimal small motion without moving the endeffector. On the other hand, assembly modes are the different solutions to the direct kinematic problem (DKP), allowing to calculate the pose of the endeffector for given drive positions. Dividing these assembly modes, there are singularities of second type, in which an infinitesimal small movement of the endeffector is possible, while all actuators are unmoved. Each combination of these working and assembly modes (called configuration) has a corresponding workspace.

For the Triglidge-structure Fig. 2 shows the two largest of these configuration workspaces (out of a total of 14). If it is

possible to change between these two a resulting overall workspace can be achieved also shown in Fig. 2. To accomplish this change several other configuration workspaces and the separating singularities have to be passed. While for first type singularities such a passing can be managed easily using joint space interpolation the passing of singularities of second type needs special considerations, since the platform's pose cannot be controlled by the drives in such a singularity. To overcome this problem we proposed an approach using gravity [12] to impose a defined movement on the platform while being in the singularity. The necessary steps and an adapted control strategy allowing for a successful realization of this approach are given in [13].

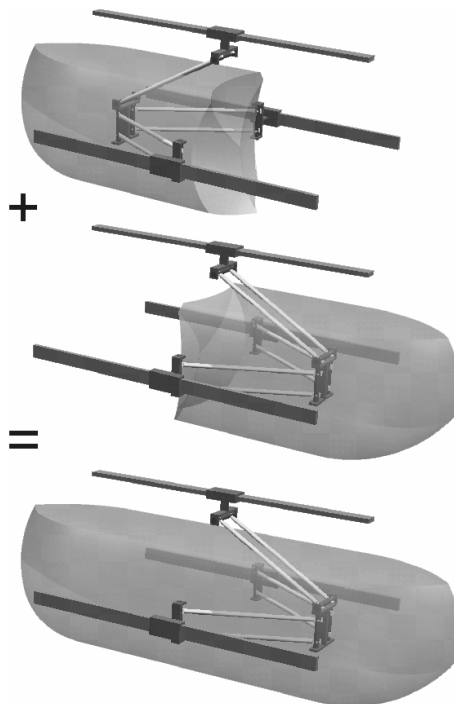


Fig. 2. Configuration workspaces and resulting overall workspace for Triglidge-structure.

Due to the time necessary for such a change between workspaces it will not be efficient to conduct this transition in every motion cycle. But it is well suited for tasks, which only require an occasional configuration change. E.g. it is reasonable to use this kind of workspace enlargement for robots handling parts from two feeders. Or it is possible to position peripheral devices, such as automatic tooling systems, in one workspace, while working in the other one. It is also very important to mention that the two used configuration workspaces itself contain no further singularities of the second type.

IV. OPTIMIZATION

A. Requirements

The Triglidge-robot is developed as a test bed within the Collaborative Research Centre SFB 562 [14] at the Technical University of Braunschweig. According to the

main topic of this interdisciplinary research group the robot is designed for high speed handling and assembly tasks. Resulting from this application area the main requirements are a large workspace to installation-space ratio (to be even improved by using the described workspace enlargement approach) and the ability for highly dynamic movements. Using a max. acceleration of the working platform of 10 g a max. platform speed of 5 m/s is to be realized for a payload of 3 kg. The payload's max. inertia around the z-axis of 0.012 kgm² has to be accelerated with 16000 °/s² up to a max. rotational speed of 1200 °/s.

B. Boundary Conditions

In the search for an optimal set of kinematic parameters several constraints are considered:

- The Triglidge-structure's kinematic properties are described using the parameters b_i, l_i, r_i ($i \in \{1,2,3\}$) as introduced in Fig. 1.
- To obtain a structure symmetrical to the x-z-plane $b_1 = b_2, l_1 = l_2$ and $r_1 = r_2$ are set.
- To further reduce the number of parameters l_1 is chosen as a reference parameter to which all others are scaled.
- The parameters are only varied in certain ranges to account for design constraints. E.g. for the y-extension of the working platform (defined by $r_1 + r_2$) a minimum value is set to allow for a central positioning of the serial drive between the joints at the platform.
- Due to the parallel arrangement of the linear drives the structure's attributes are not dependent on the x-position of the platform (except for areas at both ends of the workspace's x-extension). Thus the optimization will be performed for a cross-section of the workspace parallel to the y-z-plane.
- While passing through a singularity of the first type (to change the configuration workspace) of chain 1 the platform must not collide with the linear guide of chain 2 and vice versa. To account for this, it is necessary to fulfill $b_1 + b_2 \geq l_1 + r_1 + r_2$.
- To minimize installation space $b_1 + b_2 = l_1 + r_1 + r_2$ is chosen.
- To avoid a cantilevered design of carriage 3 (described by a large value a_3) the workspace is limited at the top by imposing $z_E \leq b_3 - r_3$ on the z-coordinate of platform point E.

C. Optimization Criteria

The following criteria are used to find an optimal set of kinematic parameters. Since both of the configuration workspaces that are going to be used are symmetrical the optimization is performed for just one of them.

- The area of a rectangular workspace in the y-z-plane is to be maximized.
- The portion of this workspace below the y-axis is to be maximized since this part of the workspace can be accessed best.

- The transmission ratio between an arbitrarily directed force \mathbf{f}_L applied to point E of the platform and the resulting force $f_{q,i}$ on drive i is to be below a value of 2 for every drive.
- The transmission ratio between a force \mathbf{f}_L directed arbitrarily parallel to the x-y-plane and applied to point E of the platform and the resulting force $f_{q,i}$ on drive i is to be below a value of 1.4 for every drive.

These last two criteria are used to limit the drive forces necessary to reach the max. acceleration of the working platform. The reason behind this limitation is that direct linear drives (which will be used as explained in section V) are only available up to certain drive forces for the desired velocities. When the drive forces necessary for a given acceleration of the platform are calculated they strongly depend on the named transmission ratio. The additional limitation on forces parallel to the x-y-plane accounts for the following assumption: If the Triglidge-structure is used for pick-and-place operations, the distance, that the payload has to be translated parallel to the x-y-plane, will (in most cases) be larger than the short stroke in z-direction to pick up or put down the payload. Hence, the acceleration periods parallel to the x-y-plane may be longer than those in z-direction. Thus, the drives should not be loaded close to their peak force (which can be exerted for a short time only) when moving the structure parallel to the x-y-plane.

D. Optimization Result

The simple build-up of the structure with only translational platform movement facilitates setting up the necessary kinematic equations (IKP, DKP and the corresponding Jacobian matrices) for the calculation of the named criteria as described for example in [15]. Using a multi-criterion approach a set of optimal kinematic parameters is calculated, which can be found in Table I.

The length of the moving range of the drives (given by $q_{max} - q_{min}$) is chosen just long enough to safely allow for the singularity passing necessary for the planned configuration change. Thus, the overlapping between the two configuration workspaces shown in Fig. 2 is kept low, resulting in an optimal improvement of workspace to installation-space ratio by the use of the described workspace enlargement approach.

TABLE I
KINEMATIC PARAMETERS OF TRIGLIDGE-ROBOT

Symbol	Unit	Values of prototype	Standardized values for benchmark
$l_1 = l_2 = l_3$	mm	600	1000
$a_1 = a_2 = a_3$	mm	105	175
$b_1 = b_2$	mm	379	631.67
b_3	mm	415	691.67
$r_1 = r_2$	mm	79	131.67
r_3	mm	110	183.33
$e_1 = e_2 = e_3$	mm	50	83.33
$[q_{min}, q_{max}]$	mm	[-640, 640]	[-1066.67, 1066.67]

V. DESIGN ISSUES

To allow for the planned passing of singularities the structure is specifically optimized for it. The chosen arrangement of the three linear guides in the base with parallel axes of the first joints on carriages 1 and 2 (see Fig. 1) facilitates a passing of all encountered singularities without any inner collisions. Furthermore it enables the structure to change its configuration without a change in platform orientation, which is important for executing the same application in all configuration workspaces. The kinematic chains have to be adapted also. A specific joint design makes the necessary movements (requiring joint angles up 180°) possible. As a compromise the chosen arrangement of the kinematic chains demands for a chain build-up able to transmit moment loads, since a rotation of the platform around the z-axis can only be inhibited by the upper chain resulting in moment loads in this chain for platform positions in the lower part of the workspace (small values for z). This increases the mass of the moved parts, which otherwise has been minimized by application of light-weight design principles. For the build-up of the kinematic chains an over-constrained design has been chosen (as explained in [12]) for stiffness reasons. It requires several of the joint axes within one kinematic chain to be parallel.

For the actuation of the three identical chains linear direct drives are chosen. Spindle drives cannot be used, because they cannot reach the maximum velocity required for the robot. Belt drives are also excluded as their lower compliance results in a higher oscillation tendency at high accelerations. The chosen drives are of an ironless design to reduce the mass of the moved parts. Fig. 3 shows the actual design of the robot.

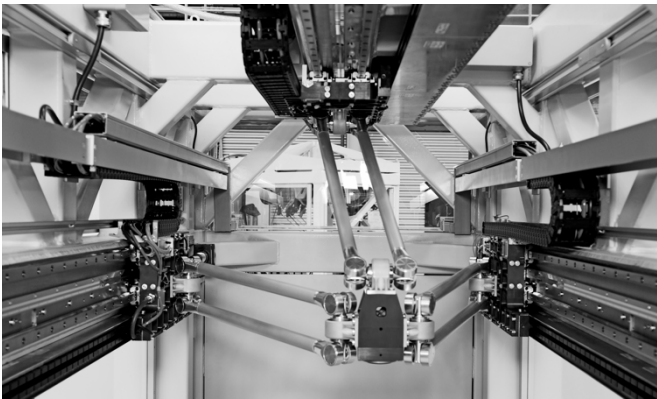


Fig. 3. Prototype of Triglide-robot.

VI. BENCHMARK DATA

The aim of this section is to provide performance data of the Triglide-structure for a joint effort of several authors to compare different structures driven by linear actuators. To allow for this each author characterizes the presented structure using standardized benchmark criteria. In this benchmark only the kinematic structures will be compared neglecting the concrete design and the attributes of the

components of each machine. For this the structures will be scaled to a rod length of 1000 mm (see Table I). For stiffness calculations standardized component properties will be used as given in Table II. The base structure, the drive carriages, the drives and the working platform are assumed to be rigid.

TABLE II
STANDARDIZED COMPONENT PROPERTIES

Property	Symbol	Unit	Standardized values for benchmark
joint stiffness	k_j	N/ μ m	50
outer rod diameter	d_a	mm	50
inner rod diameter	d_i	mm	38
Young's modulus of rods	E_r	GPa	70

Except for the data on workspace all other criteria will only be given for a cross-section of the workspace parallel to the y-z-plane since the Triglide-structure's characteristic values do not change with changing x-values except for areas on both ends of the workspaces x-extension.

A. Workspace

To characterize the workspace W the workspace to installation-space ratio η is calculated. The installation space W_{inst} is defined as the volume of the smallest cuboid in which the robot can fit. It can be calculated by

$$W_{inst} = (q_{max} - q_{min})(b_1 + a_1 + b_2 + a_2)(b_3 + a_3) \quad (1)$$

with the parameters a_i accounting for the thickness of the carriages. Note that this determination of the installation space takes into account only the kinematic structure. For a real robot the resulting values will be larger, since additional moving ranges of the drives for emergency braking and the concrete design of the base structure have to be considered.

For the determination of the workspace for a given configuration of the structure a cuboid large enough to contain all possible positions of the platform is discretized. Using the IKP and DKP for the given configuration it can be tested for all elements of this cuboid whether they belong to the workspace. Summing up the volume of all elements that are part of the workspace its overall volume is calculated. Due to the constant scaling factor between the kinematic parameters of the prototype and the standardized values for this benchmark the resulting value for η is the same for both. Using just one of the configuration workspaces shown in Fig. 2 a value of $\eta = 0.52$ is calculated. But using the overall workspace resulting from the presented workspace enlargement approach this value can be nearly doubled to $\eta = 0.96$.

B. Stiffness

Due to the over-constrained build-up of the kinematic chains, an exact calculation of the structure's stiffness can only be done using finite element analysis after extensive modeling. A conservative approximation can however be

obtained as follows: For this a modified build-up of the kinematic chains is assumed having ball-joints at all the rods' ends. Since this does not allow the chains to transmit moment loads any more this modified structure will be less stiff than the real one. In fact, at the bottom of the workspace (lowest values for z) it will become singular, because none of the chains can inhibit a rotation of the platform about the z-axis. But for workspace regions away from this lower border this problem does not arise, allowing for a good estimation of the stiffest region of the workspace.

The procedure for stiffness-calculation is analog to one described in [4] for the Urane SX. It is based on the assumption that rods can only transmit forces along its axes, which is true for the modified structure with ball joints at the rods' ends if friction in the joints and dynamical forces due to the rods' masses are neglected. Thus, according to Fig. 1 the forces in the rods can be written as (with j distinguishing the two rods of chain i):

$$\mathbf{f}_{ij} = f_{ij} / l_{ij} \cdot \overline{B_{ij}C_{ij}} \quad (2)$$

If the working platform is loaded in point E with an external force \mathbf{f}_L and an external moment \mathbf{m}_L the resulting forces in the rods can be calculated by setting up the force and moment equilibrium for E:

$$\sum_{i=1}^3 \left(\sum_{j=1}^2 \mathbf{f}_{ij} \right) + \mathbf{f}_L = \mathbf{0} \quad (3)$$

$$\sum_{i=1}^3 \left(\sum_{j=1}^2 \mathbf{f}_{ij} \times \overline{C_{ij}E} \right) + \mathbf{m}_L = \mathbf{0} \quad (4)$$

$$\underbrace{\begin{pmatrix} l_{11}^{-1} \overline{B_{11}C_{11}} & l_{11}^{-1} \left(\overline{B_{11}C_{11}} \times \overline{C_{11}E} \right)^T \\ l_{12}^{-1} \overline{B_{12}C_{12}} & l_{12}^{-1} \left(\overline{B_{12}C_{12}} \times \overline{C_{12}E} \right)^T \\ l_{21}^{-1} \overline{B_{21}C_{21}} & l_{21}^{-1} \left(\overline{B_{21}C_{21}} \times \overline{C_{21}E} \right)^T \\ l_{22}^{-1} \overline{B_{22}C_{22}} & l_{22}^{-1} \left(\overline{B_{22}C_{22}} \times \overline{C_{22}E} \right)^T \\ l_{31}^{-1} \overline{B_{31}C_{31}} & l_{31}^{-1} \left(\overline{B_{31}C_{31}} \times \overline{C_{31}E} \right)^T \\ l_{32}^{-1} \overline{B_{32}C_{32}} & l_{32}^{-1} \left(\overline{B_{32}C_{32}} \times \overline{C_{32}E} \right)^T \end{pmatrix}}_{\mathbf{J}_r} \begin{pmatrix} f_{11} \\ f_{12} \\ f_{21} \\ f_{22} \\ f_{31} \\ f_{32} \end{pmatrix} = \begin{pmatrix} \mathbf{f}_L \\ \mathbf{m}_L \end{pmatrix} \quad (5)$$

With (5) being the matrix notation. So, with \mathbf{J}_r not being singular the forces in the rods due to an external load are:

$$\mathbf{f}_r = \mathbf{J}_r^{-1} \begin{pmatrix} \mathbf{f}_L \\ \mathbf{m}_L \end{pmatrix} \quad (6)$$

Next, the change of length Δr_{ij} of each rod due to a force on the rod can be evaluated using its stiffness $k_{r,ij}$.

$$f_{ij} = k_{r,ij} \Delta r_{ij} \quad (7)$$

Using Hooke's law for each rod and considering the joints of stiffness k_j at each end of it a rod's stiffness can be calculated using:

$$\left(k_{r,ij} \right)^{-1} = k_j^{-1} + \left(\frac{(d_a^2 - d_i^2) \pi E_r}{4l_{ij}} \right)^{-1} + k_j^{-1} \quad (8)$$

For all rods it can be written in matrix form:

$$\Delta \mathbf{r} = \mathbf{K}_r^{-1} \mathbf{f}_r \quad (9)$$

$$\mathbf{K}_r = \text{diag} \left(\left[k_{r,11} \quad k_{r,12} \quad k_{r,21} \quad k_{r,22} \quad k_{r,31} \quad k_{r,32} \right] \right) \quad (10)$$

Due to such a change of length of the rods the platform will undergo a translation $\Delta \mathbf{x}_r$ and a rotation $\Delta \mathbf{\alpha}_r$. For small values of this displacement it can be connected to the external load on the platform using the principle of virtual work:

$$\begin{pmatrix} \mathbf{f}_L \\ \mathbf{m}_L \end{pmatrix}^T \begin{pmatrix} \Delta \mathbf{x}_r \\ \Delta \mathbf{\alpha}_r \end{pmatrix} = \mathbf{f}_r^T \Delta \mathbf{r} \quad (11)$$

Using (6) this derives to

$$\begin{pmatrix} \mathbf{f}_L \\ \mathbf{m}_L \end{pmatrix} = \mathbf{J}_r \mathbf{K}_r (\mathbf{J}_r)^T \begin{pmatrix} \Delta \mathbf{x}_r \\ \Delta \mathbf{\alpha}_r \end{pmatrix} = \mathbf{K} \begin{pmatrix} \Delta \mathbf{x}_r \\ \Delta \mathbf{\alpha}_r \end{pmatrix} \quad (12)$$

giving the necessary external load to reach a given displacement of the platform with \mathbf{K} being the stiffness matrix of the structure.

Table III shows the structure's stiffness in x-, y- and z-direction calculated as the ratio between the necessary force and the resulting displacement for each of the Cartesian directions. Note, that this does not include the external moment which is also necessary to cause this displacement. Since the stiffness is dependent on the platform's position in the workspace the minimum, maximum and average values over the entire y-z-cross-section of the workspace are given. Additionally, Table III shows the same values for a subspace of the workspace which can be seen in Fig. 4 featuring the best 70% of the values of the stiffness in x-direction.

TABLE III
CARTESIAN STIFFNESS IN N/ μm

	Entire WS			Best 70% of WS		
	x	y	z	x	y	z
minimum	33	17	6	65	17	6
average	69	29	25	74	26	19
maximum	81	47	58	81	43	48

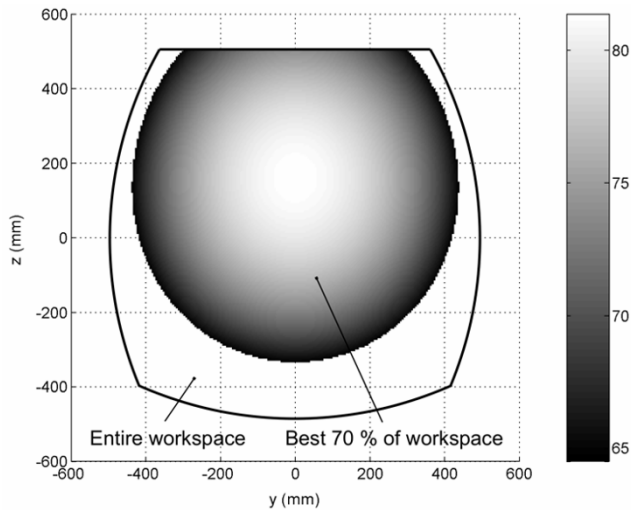


Fig. 4. Stiffness in x-direction (N/μm) for y-z cross-section of workspace.

C. Sensitivity to changes in rod length

The criteria described above were calculated for the nominal lengths of the links. Due to manufacturing tolerances it is not possible to built a machine exactly according to the nominal values, which makes the influence of link length errors another point of interest. Thus, for the rods (being the longest links) the influence of a change of their length Δr on the platform’s position and orientation is calculated.

As in the previous subsection a modified structure with ball joints at the rod’s ends is considered. Starting from (11) based on the principle of virtual work and using (6) the following correlation can be found:

$$\begin{pmatrix} \Delta \mathbf{x}_r \\ \Delta \mathbf{a}_r \end{pmatrix} = (\mathbf{J}_r^T)^{-1} \Delta \mathbf{r} \quad (13)$$

For the six rods Table IV shows the resulting translational displacement of the platform due to a change of 1 μm for each rod’s length l_{ij} . Over the subspace of the workspace featuring the best stiffness values in x-direction (defined in the previous subsection) the minimum, maximum and average displacements are given.

TABLE IV
TRANSLATIONAL PLATFORM DISPLACEMENT (μm) DUE TO CHANGE IN LENGTH OF ROD l_{ij} OF 1 μm FOR BEST WORKSPACE (X-STIFFNESS)

	l_{11}	l_{21}	l_{21}	l_{22}	l_{31}	l_{32}
minimum	0.9	1.0	0.9	1.0	0.9	0.9
average	1.4	1.7	1.4	1.7	1.7	1.7
maximum	2.0	2.1	2.0	2.1	2.5	2.5

VII. CONCLUSION

The development of the robot presented in this paper is focused on two main aspects. On the one hand the advantages of parallel kinematic structures are used to design a robot for highly dynamic applications. With a payload of

up to 3 kg it not only allows for the fast handling of very small parts but also for more demanding operations requiring e.g. more complex (and thus heavier) gripping technology. On the other hand one of the main drawbacks of parallel structures is tackled by using two configuration workspaces to get a significantly larger overall workspace at the same installation space. The described structure optimization with its optimization criteria reflects these two focal points.

The final dimensions of the structure’s are evaluated regarding workspace to installation-space ratio, Cartesian stiffness and sensitivity to changes in rod length. Using standardized component attributes these values will be used to do a benchmark of several parallel kinematic structures all driven by linear actuators.

REFERENCES

- [1] R. Clavel, “Robots Parallèles,” *Techniques de l’Ingénieur, traité Mesures et Contrôle*, vol. R 7 710, 1994, pp. 1-8.
- [2] M. Hebsacker, T. Treib, O. Zirn, and M. Honegger, “Hexaglide 6 DOF and Triaglide 3 DOF parallel manipulators,” *Parallel Kinematic Machines*, C. R. Boër, L. Molinari-Tosatti and K. S. Smith (eds), London: Springer, 1998, pp. 345-355.
- [3] G. Pritschow and K.-H. Wurst, “Systematic design of Hexapods and other parallel link systems,” *Annals of the CIRP*, 1997, pp. 291-295.
- [4] O. Company, F. Pierrot, F. Launay and C. Fioroni, “Modeling and preliminary design issues for 3-Axis parallel machine-tool,” in *Proc. Parallel Kinematic Machines Int. Conf.*, Ann Arbor, MI (USA), 2000, pp. 14-23.
- [5] T. Brogardh, S. Hanssen and G. Hovland, “Application-oriented development of parallel kinematic manipulators with large workspace,” in *Proc. 2nd Int. Colloquium of the Collaborative Research Center 562*, Braunschweig (Germany), 2005, pp. 153-170.
- [6] D. N. Nenchev, S. Bhattacharya and M. Uchiyama, “Dynamic analysis of parallel manipulators under the singularity-consistent parameterization,” *Robotica*, vol. 15, 1997, pp. 375-384.
- [7] P. Wenger and D. Chablat, “Workspace and assembly modes in fully-parallel manipulators: A descriptive study,” in *Proc. Int. Symposium on Advances in Robot Kinematics*, Strobl, Salzburg (Austria), 1998, pp. 117-126.
- [8] J. Hesselbach, M. Helm and S. Soetebier, “Connecting assembly modes for workspace enlargement,” *Advances in robot kinematics Theory and applications*, J. Lenarčič and F. Thomas (eds), Dordrecht (Netherlands): Kluwer Academic Publishers, 2002, pp. 347-356.
- [9] F. Bleicher, “Optimizing a three-axes machine-tool with parallel kinematic structure,” in *Proc. 3rd Chemnitz Parallel Kinematics Seminar*, Chemnitz (Germany), 2002, pp. 883-894.
- [10] I. Bonev, *Kinematics terminology related to parallel mechanisms*, <http://www.parallemic.org/Terminology/Kinematics.html>, 2002
- [11] C. Gosselin and J. Angeles, “Singularity analysis of closed-loop kinematic chains,” *IEEE Trans. on Robotics and Automation*, no. 6, vol. 3, 1990, pp. 281-290.
- [12] C. Budde, P. Last and J. Hesselbach, “Workspace enlargement of a Triglode robot by changing working and assembly mode,” in *Proc. of IASTED Int. Conf. on Robotics and Applications*, Cambridge, MA (USA), 2005, pp. 244-248.
- [13] J. Maaß, M. Kolbus, C. Budde, J. Hesselbach and W. Schumacher, “Control strategies for enlarging a spatial parallel robot’s workspace by change of configuration,” in *Proc. 5th Chemnitz Parallel Kinematics Seminar*, Chemnitz (Germany), 2006, pp. 515-530.
- [14] M. Krefft, M. Frindt, J. Hesselbach and F. M. Wahl, “Robotic systems for handling and assembly,” in *CD-Proc. Workshop on Fundamental Issues and Future Research Directions for Parallel Mechanisms and Manipulators*, Quebec City (Kanada), 2002.
- [15] M. Stock and K. Miller, “Optimal kinematic design of spatial parallel manipulators: Application to linear Delta robot,” *Trans. of the ASME*, vol. 125, June 2003, pp. 292-301.